

# PID Parameters Auto-Tuning on GPS-based Antenna Tracker Control using Fuzzy Logic

Ahmad Riyandi<sup>\*)</sup>, Sumardi, Teguh Prakoso

Department of Electrical Engineering, Faculty of Engineering, Diponegoro University  
Jl. Prof. Soedarto, SH, Kampus Undip Tembalang, Semarang, Indonesia 50275

---

**Citation:** A. Riyandi, S. Sumardi, and T. Prakoso, "PID Parameters Auto-Tuning on GPS-based Antenna Tracker Control using Fuzzy Logic," Jurnal Teknologi dan Sistem Komputer, vol. 6, no. 3, Jul. 2018. doi: 10.14710/jtsiskom.6.3.2018.122-128, [Online].

---

**Abstract** – Moving vehicles require an antenna to communicate which is placed on the vehicles and at the ground station (ground control station, GCS). Generally, GCS uses a directional antenna equipped with the drive system with the conventional proportional, proportional-integral, or proportional-integral-derivative (PID) control, and step-tracking algorithms based on the received signal strength indicator (RSSI). This research used PID control method tuned with fuzzy logic based on Global Positioning System (GPS) to control a directional antenna at GCS. The resulting antenna tracker system was capable of tracking objects with a minimal error of 0° at azimuth and elevation angle and had a maximal error of 49° for a 49 km/hour speed object. The system had an average rise time of 0.7 seconds at an azimuth angle and 1.08 seconds at an elevation angle. This system can be used to control antenna direction for moving vehicles, such as an unmanned aerial vehicle (UAV) and rocket.

**Keywords** – antenna tracker; GPS; self-tuning fuzzy-PID; UAV communication

## I. INTRODUCTION

Vehicles that have wide-ranging areas such as rockets, satellites, or unmanned aerial vehicles (UAVs) require an antenna to communicate. The antenna is placed on the vehicles and at the ground control station (GCS). Some efforts are needed to improve the quality of communication between the vehicles and GCS. Improvement on the side of the vehicles is usually avoided because it can increase the vehicles load.

Improvement on the GCS side that can be done is using a directional antenna and moving the antenna facing the vehicles [1]. Generally, the vehicles use the omnidirectional type of antenna, meaning that radiation patterns are spread evenly in all directions [2]-[4]. The directional antenna on the GCS has a radiation pattern that forms a beam in a particular direction, while in the other direction the signal is weak. The use of a

directional antenna extends the signal range and optimizes power consumption [5], [6].

The common method used to track the vehicles is with real-time global positioning system (GPS) data as a reference or using the received signal strength indicator (RSSI). Tracking method using GPS aims to get the coordinate of GCS and the vehicles, then process it to obtain an angle between the two [7]. The RSSI method works by determining the strong signal received by at least 2 antennas on the GCS as a reference for directing the antenna [8].

Many research and development of antenna drive systems have been done, such as a recipient of video link data from a UAV using 5 channels antenna mono pulse [8]. The researches used various control methods such as Proportional controllers [7], Proportional-Integral controller (PI) [9], Proportional-Integral-Derivative (PID) controllers [10], step-tracking algorithm with  $H_\infty$  controller for closed-loop tracking design [11], Fuzzy-PD [12], and using Fuzzy-PID [13]. All of the researches mentioned was conducted by RSSI tracking method. This method has disadvantages such as the construction of complex antennas, and susceptible to be interfered by other signals.

In this research, a PID control system was optimized by using fuzzy logic to control the antenna drive system so that the antenna always leads to a vehicle. The tracking method used GPS as a reference to improve the previous research deficiencies. The expected result of this research is the antenna can face the vehicle with high accuracy and fast response.

## II. RESEARCH METHODS

This chapter describes the components of the system and the used control methods. Generally, the antenna tracker system consists of a 433MHz Yagi-Uda antenna, an antenna drive device placed on GCS, and a payload as data sender from a vehicle to the GCS. The control method used is the optimized PID method using fuzzy logic.

The 433 MHz Yagi-Uda antenna is used because it has a directional radiation pattern. The antenna must meet several criteria, namely the standing wave ratio (VSWR)  $\leq 2$ , the reflection coefficient value of the antenna  $\leq -10$  dB, and the link budget value  $\geq 15$  dBm.

---

<sup>\*)</sup> Correspondence author (Ahmad Riyandi)  
Email: ahmad.ian.riyandi@gmail.com

**Table 1.** CST Studio Suite antenna simulation results

No.	Criteria	Expected Results	Results
1	Voltage Standing Wave Ratio (VSWR)	$1 < \text{VSWR} < 2$	1.078
2	Reflection coefficient	$< -10 \text{ dB}$	-28.436 dB
3	Impedance	$50 \Omega$	$49.352 \Omega$
4	Gain	10 dB	10 dB

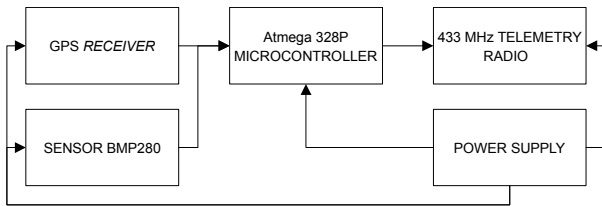


**Figure 1.** Block diagram of the data sender device

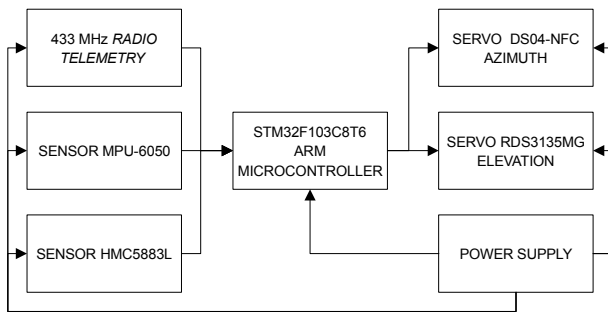


**Figure 2.** Block diagram of the antenna drive device

To meet these criteria, antennas are designed and simulated using CST Studio Suite application. New antennas can be produced after the simulation results meet these criteria. The simulation results of the antenna used in this research are shown in Table 1.

The data sender composed of several components as shown in Figure 1. This data sender device serves to send the location data of the vehicle to the antenna drive device in real-time. The location information of the vehicle is obtained through readings of BMP280 barometric sensors and GPS receivers. The BMP280 barometric sensor reads the altitude of the vehicles, while the GPS receiver reads the latitude and longitude data of the vehicle. The vehicle location information is sent to the antenna control device via 433 MHz telemetry radio. All components are supplied by a power supply system consisting of a 7.4 V battery and a voltage regulator.

The antenna drive device is generally composed of several components as shown in Figure 2. Two servo motors are used each as an antenna drive at an azimuth angle and an elevation angle. The actual angular of the antenna in the azimuth direction is read by the HMC5883L magnetometer sensor, and in the elevation direction read by the MPU-6050 sensor. A 433 MHz

telemetry radio connected to a 433 MHz Yagi-Uda antenna is used to receive the vehicle location information. The location data is processed by the STM32F108C microcontroller into an input reference for this antenna tracking system. The voltage supply system consists of an 11.1 V battery and some voltage-reducing regulator.

The input reference of the antenna drive consists of two inputs, namely the azimuth setpoint and the elevation setpoint. The azimuth setpoint value is obtained using the bearing equation whose output is the azimuth angle. Calculation of bearing angle using Equation 1 to Equation 4. Parameter  $z$  denotes azimuth angle,  $\lambda_a$  as longitude of GCS,  $\lambda_o$  as longitude of the vehicle,  $\phi_a$  as latitude of GCS, and  $\phi_o$  as latitude of the vehicle.

$$X = \cos \phi_o * \sin \Delta \lambda \quad (1)$$

$$Y = \cos \phi_a * \sin \phi_o - \sin \phi_a * \cos \phi_o * \cos \Delta \lambda \quad (2)$$

$$\Delta L = \lambda_o - \lambda_a \quad (3)$$

$$z = \text{atan}(X, Y) \quad (4)$$

The elevation setpoint value is derived from triangular trigonometric calculations, using altitude and distance values from GCS to the object projection point on the earth's surface (Haversine). The calculations of Haversine are calculated using Equation 5 to Equation 9.  $R$  denotes the radius of the earth (6,371 km) and  $d$  as Haversine. Equation 10 is a trigonometric equation to obtain an elevation angle where  $b$  is the elevation angle and  $f$  is the altitude of the vehicle.

$$\Delta \phi = \phi_2 - \phi_1 \quad (5)$$

$$\Delta \lambda = \lambda_2 - \lambda_1 \quad (6)$$

$$a = \sin^2\left(\frac{\Delta \phi}{2}\right) + \cos \phi_1 * \cos \phi_2 * \sin^2\left(\frac{\Delta \lambda}{2}\right) \quad (7)$$

$$c = 2 * \text{atan}(\sqrt{a}, \sqrt{1-a}) \quad (8)$$

$$d = R * c \quad (9)$$

$$b = \tan^{-1}\left(\frac{d}{f}\right) \quad (10)$$

From the reference value, the value of error and  $\Delta$ error can be found as in Equations 11 and Equation 12. Parameter  $e(k)$  denotes actual error and  $e(k-1)$  as previous error.

$$e(k) = \text{Setpoint} - \text{Actual angle} \quad (11)$$

$$\Delta e(k) = e(k) - e(k-1) \quad (12)$$

The error and  $\Delta$ error values are used as inputs for the fuzzy self-tuning PID control method as shown by the block diagram of Figure 3. Based on the mathematical equations of PID, the discrete version embedded in the digital system will have the form as seen in Equation 13 to Equation 16 where  $U_p(k)$ = proportional control,  $U_i(k)$ = integral control,  $U_d(k)$ = derivative control, and  $U(k)$  = PID control.  $K_p$ ,  $K_i$ , and  $K_d$  are PID control parameters tuned using fuzzy logic.

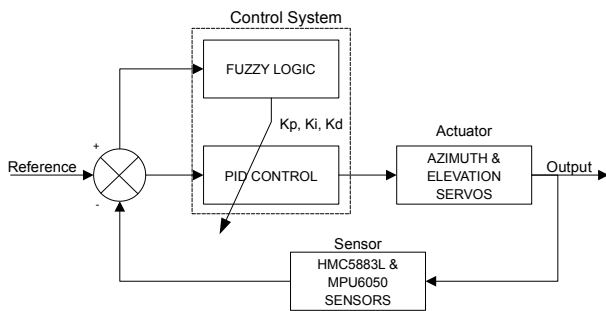


Figure 3. Control system block diagram

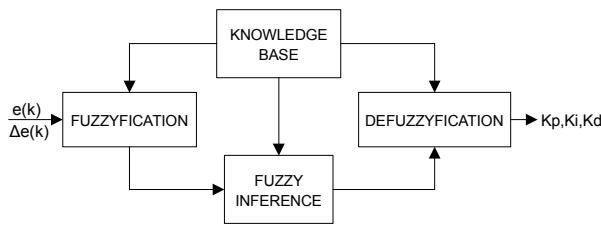


Figure 4. Fuzzy logic block diagram

$$U_p(k) = K_p \cdot e(k) \quad (13)$$

$$U_i(k) = U_i(k-1) + K_i \cdot T_c \cdot e(k) \quad (14)$$

$$U_d(k) = K_d \frac{\Delta e(k)}{T_c} \quad (15)$$

$$U(k) = U_p(k) + U_i(k) + U_d(k) \quad (16)$$

The use of fuzzy logic aims to optimize the output of the PID. The expected result of this control is that the system is capable of achieving set points in the shortest time possible without overshoot and oscillation.

In Fuzzy logic processing, there are several stages as in Figure 4. The first stage is the fuzzification. This stage is the fuzzy set determination of the membership function graph. The graph of membership functions designed on this system consists of three triangular membership functions and two trapezoidal membership functions. The five membership functions are each labeled NB, N, Z, P, and PB.

Membership function used in this system is divided into membership function for *error* input and membership function for *Δerror* input. The membership function for *error* input limitation on the x-axis is based on the maximum error that may occur on the system, while the membership function for *Δerror* input limit is based on the observation of the maximum value of *Δerror* that can occur in the system. The y-axis on the membership function graph is the degree of membership. In this system, the degree of membership used is from 0 to 1. The degree of membership is obtained through the mathematical equation of the trapezoidal or triangular membership function. The membership function at the elevation angle input is shown in Figure 5 and Figure 6, while the membership function at the azimuth angle is shown in Figure 7 and Figure 8.

The knowledge base consists of a database and a rule

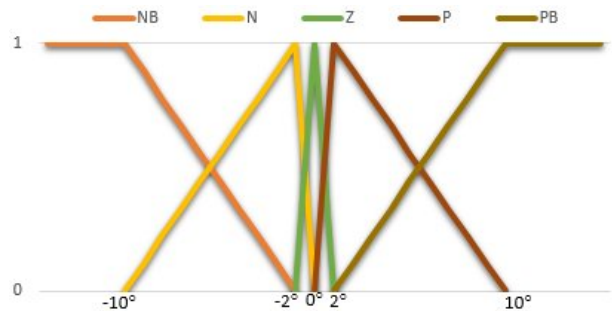


Figure 5. Input membership function for elevation angle error

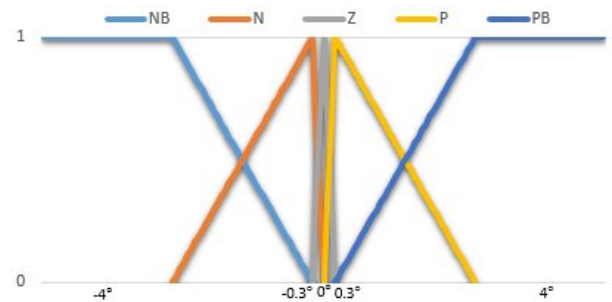


Figure 6. Input membership function for elevation angle Δerror

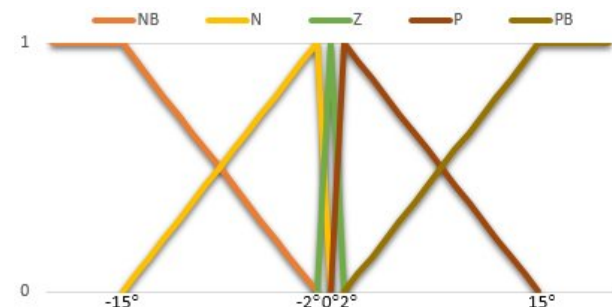


Figure 7. Input membership function for azimuth angle error

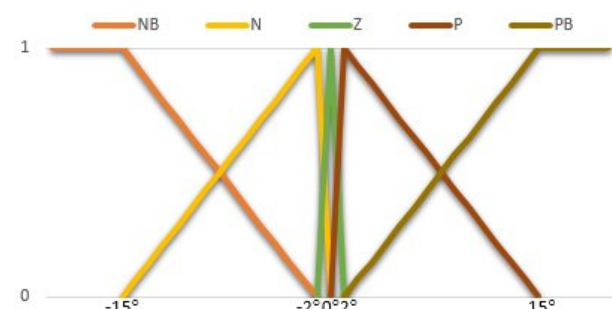


Figure 8. Input membership function for azimuth angle Δerror

base. The fuzzy logic rule base is obtained using the heuristic approach, where the rule base is obtained from the analysis of the effect of PID parameters on the transient response of the system to obtain the desired system response. The set rule is used to connect between input variables and output variables. This used

**Table 2.** Rule base for Kp at elevation and azimuth angle

<i>Error</i> $\Delta Error$	NB	N	Z	P	PB
NB	KS	B	B	K	B
N	K	B	B	K	BS
Z	BS	S	S	S	BS
P	BS	K	B	B	K
PB	B	K	B	B	KS

**Table 3.** Rule base for Ki at elevation and azimuth angle

<i>Error</i> $\Delta Error$	NB	N	Z	P	PB
NB	KS	B	B	K	B
N	K	B	B	K	BS
Z	BS	S	S	S	BS
P	BS	K	B	B	K
PB	B	K	B	B	KS

**Table 4.** Rule base for Kd at elevation and azimuth angle

<i>Error</i> $\Delta Error$	NB	N	Z	P	PB
NB	BS	B	B	K	KS
N	B	B	B	K	KS
Z	S	S	S	S	S
P	KS	K	B	B	B
PB	KS	K	B	B	BS

the IF-THEN rules. The rules base for this system is shown in Tables 2 to Table 4 which contains variables KS, K, S, B, BS, or called singleton. The singleton value is derived from tuning the PID parameters using the trial and error method.

The next stage in fuzzy logic processing is fuzzy inference or decision-making system. At this stage, the decision-making method used is the Sugeno method. The process of obtaining a firm value from the fuzzy set occurs in the defuzzification process. The method used in defuzzification is the weighted average method with the formula as in Equation 17, where  $Z$  is the result of the rule evaluation process, while  $Z_n$  is the singleton value on the  $n$ th label of the linguistic variable of the output membership function.  $W_n$  is the degree of fuzzy output membership. The number of  $W_n$  is equal to the number of  $Z_n$ , that is as many fuzzy sets are designed on the output membership function.

$$Z = \sum_{n=1}^n \frac{W_n Z_n}{W_n} \quad (17)$$

### III. RESULTS AND DISCUSSION

System testing was done through several stages. The first stage of testing was done on each sensor and GPS used. The next stage was testing the system response

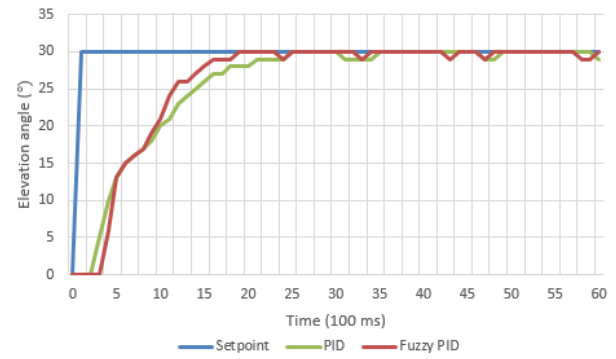


**Figure 9.** System response at the elevation angle with setpoint is 30°.

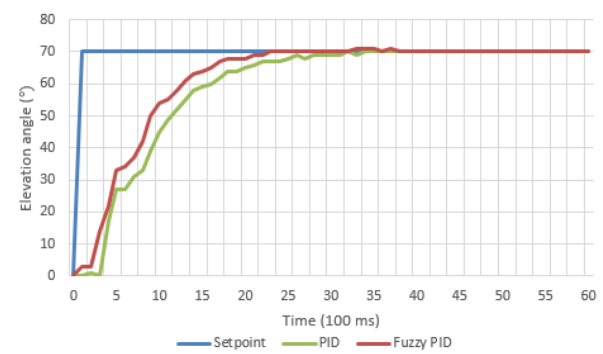


**Figure 10.** System response at the elevation angle with setpoint is 70°.

**Table 5.** System response at the various elevation angle

Set No	point (°)	Rise Time (seconds)		
		Conventional PID	PID self-tuning fuzzy	Difference
1	10	2.5	2.1	0.4
2	30	2.6	1.9	0.7
3	70	3.2	2.3	0.9
Average		2.76	2.1	0.67

**Table 6.** System response at the various azimuth angle

Set No	point (°)	Rise Time (seconds)		
		Conventional PID	PID self-tuning fuzzy	Difference
1	30	1.4	0.7	0.7
2	90	1.4	0.8	0.6
3	180	1.9	1.2	0.7
4	210	1.4	1.2	0.2
5	270	1.5	0.9	0.6
Average		1.52	0.96	0.56

with manual input. The last stage was testing the whole system by laying objects on certain vehicles.

The sensor testing parameter is the level of accuracy. The magnetometer and MPU sensor tests were

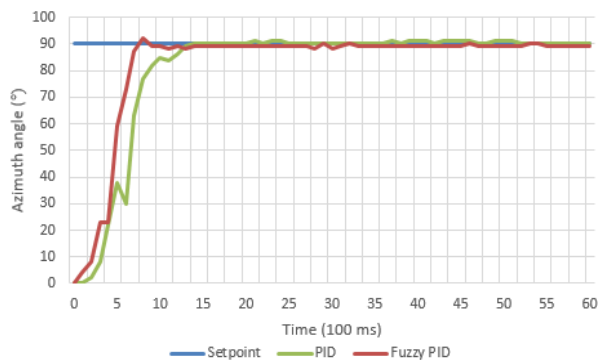


**Figure 11.** System response at the azimuth angle with setpoint is  $90^\circ$

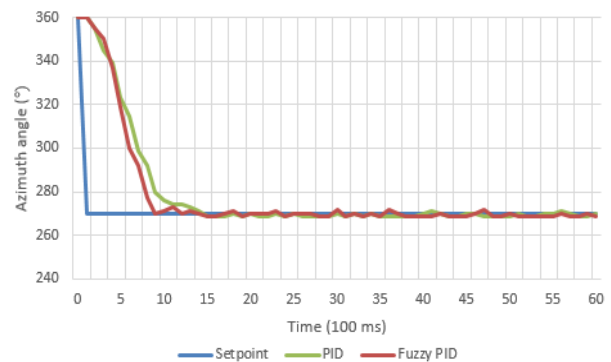


**Figure 13.** System response at the azimuth angle with setpoint is  $210^\circ$

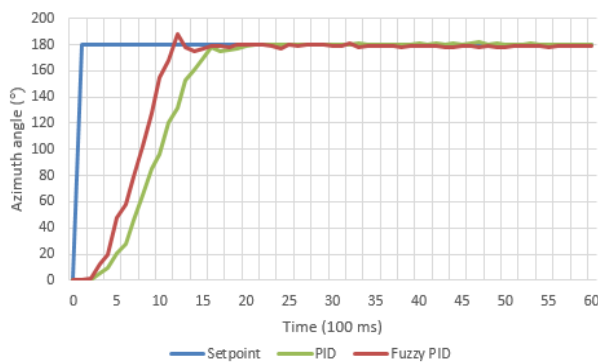


**Figure 12.** System response at the azimuth angle with setpoint is  $180^\circ$

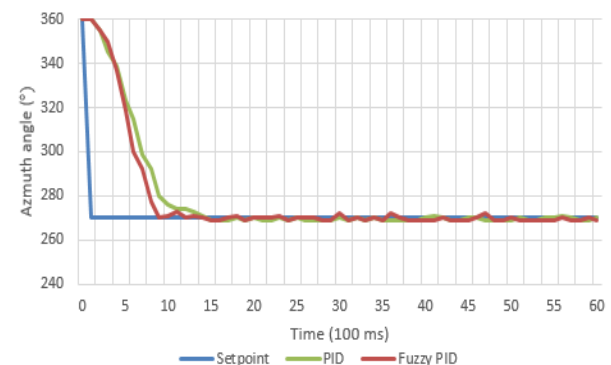


**Figure 14.** System response at the azimuth angle with setpoint is  $270^\circ$

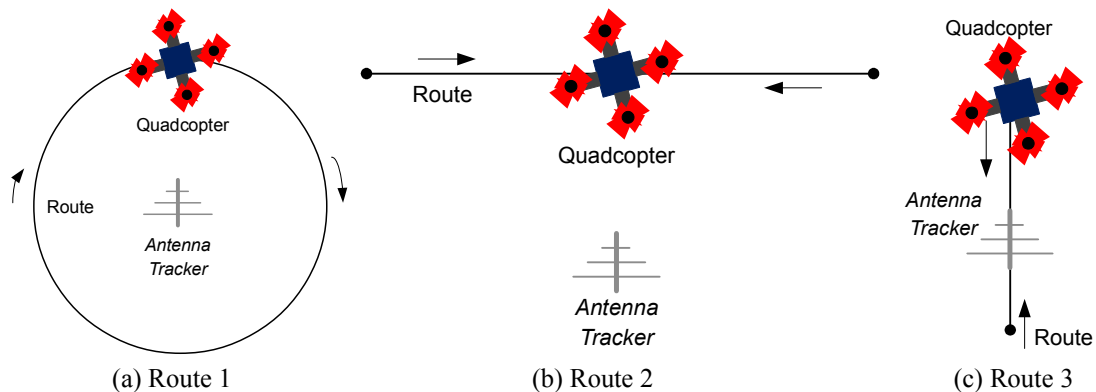


**Figure 15.** Quadcopter routes for system testing

performed using a protractor as a reference. Testing of barometric sensors and GPS used benchmark data as a reference. The test results showed that an average magnetometer sensor error rate of  $8.4^\circ$ , MPU  $0.3^\circ$ , and GPS 5 meters. From the test results, it was decided that the error rate is still within reasonable limits, so that can be continued to test the system response.

System response test was done to measure the performance of fuzzy logic to the used control system. The test was performed on the servo elevation with setpoint  $30^\circ$  and  $70^\circ$  as shown in Figure 9 and Figure 10, and on the azimuth servo with various setpoints as shown in Figure 11 to Figure 14. The test results are summarized in Table 5 and Table 6. The fuzzy logic was able to optimize PID control. This is evidenced by test

data showing that fuzzy logic is able to speed up the system to reach the setpoint. The result of the system response showed that fuzzy logic can optimize PID control with the better rise time to the steady state than conventional used in [7], [9] and [10].

The last stage of this test was to test the system by laying objects on certain vehicles. The first test was done by laying the object on a quadcopter so that the object's velocity and object's distance cannot be measured. The test route is shown in Figure 15. The data of the three trials are summarized in Table 7 and Table 8. It showed that the system can follow the object on variations of the tested route. This was evidenced by the minimum error value of all experiments is  $0^\circ$ . The system can also follow objects without data loss despite

**Table 7.** Routing response at the elevation angle changes

No	Route	Rise time (seconds)	Max. error (°)	Min. error (°)	Avg. error (°)
1	Route 1	1	38	0	6.47
2	Route 2	1.08	36	0	3.27
3	Route 3	1	38	0	9.6

**Table 8.** Routing response at the azimuth angle changes

No	Route	Rise time (seconds)	Max. error (°)	Min. error (°)	Avg. error (°)
1	Route 1	0.5	91	0	9.76
2	Route 2	0.7	83	0	4.4
3	Route 3	0.4	76	0	10.2

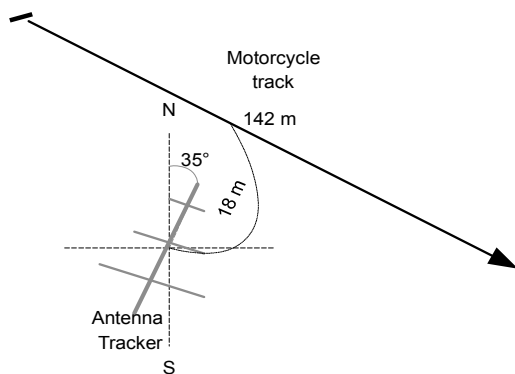


**Figure 16.** Motorcycle driven route

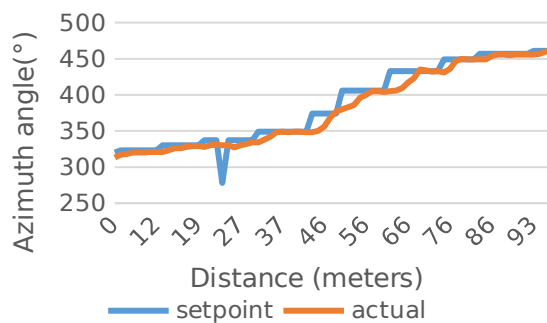


**Figure 17.** Azimuth angle response at speed 20 kmph

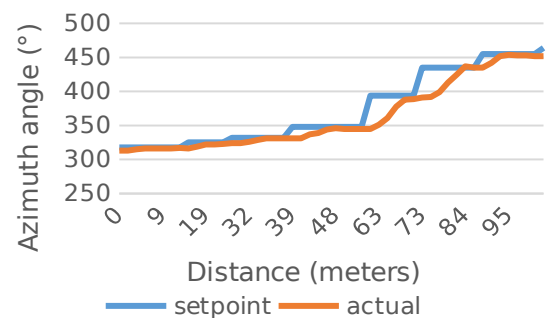


**Figure 18.** Azimuth angle response at speed 40 kmph

**Table 9.** Azimuth servo response for the various speed movement

No	Speed (km/h)	Time (seconds)	Max. error (°)	Min. error (°)	Avg. error (°)	Penalty (dB)
1	20	14.4	19	0	2.4	2.22
2	40	7.3	28	0	6.8	-1.89
3	60	5.6	49	0	9.3	6.37

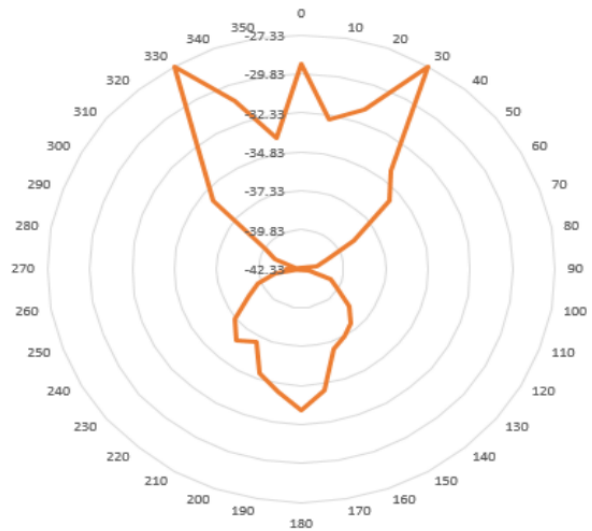


**Figure 19.** Antenna radiation pattern at the azimuth angle

having a maximum error of up to 91° at azimuth angle and 38° at elevation angle. The maximum value of these errors occurs because the quadcopter changes direction drastically before GPS updates its data. This research performed better routing response at both elevation and azimuth angle changes than [7] which results in 8,3 of average error of the antenna using the RSSI method.

The second test was done by laying the object on a motorcycle so that the speed and distance of the object can be measured. In this test the motorcycle was driven on the track as in Figure 16 with three variations of speed. The test was focused on the azimuth servo response with a test angle between 320° to 100°. The graph of the test results is shown in Figure 17 and Figure 18. The test results with measured objects are summarized in Table 9. From the three tests, it can be seen that the system can follow the object even as the speed is increased. This was evidenced by the less tracking time when the velocity was increased.

The implication of communication or penalty in the maximum error was found by calculating the signal to noise ratio (SNR) value of the antenna. The SNR calculation uses the antenna radiation pattern data as in Figure 19, where the relative strength of the antenna field at the actual position is reduced by the relative strength of the antenna field in the direction of the maximal error. Table 9 shows that the penalty at the rate of 40 kmph was negative. This happened because the

antenna radiation pattern was not ideal where the strongest relative field strength was not at an angle of  $0^\circ$  but at an angle of  $\pm 30^\circ$ . From the test results could be concluded that the increase in speed leads to an increase in average error and maximum error. This happens because the maximum value of the GPS update rate was 5 Hz which means that the position data of the object was updated at most every 0.2 seconds.

This antenna drive system control using PID tuned with fuzzy logic can track a moving vehicle with high accuracy and better responses than previous research. It had better responses to follow a moving vehicle in both elevation and azimuth direction than conventional PID in [7], [9], [10]. This system can track and control antenna direction without using the omnidirectional antenna as [2]-[4] and GPS as reference instead of using the RSSI method in [7], [8].

#### IV. CONCLUSIONS

An antenna tracker system had ability following the movement of objects with better responses. The fuzzy logic tuning was capable of optimizing PID control so that it can increase the system's average rise time at the azimuth angle and elevation angle. The system can follow objects on a variety of routes without losing data. The system was also capable of following the object with speed up to 60 kmph.

#### REFERENCES

- [1] D. Stojcsics and L. Somlyai, "Improvement Methods of Short Range and Low Bandwidth Communication for Small Range UAVs," in *IEEE 8th International Symposium on Intelligent Systems and Informatics*, Subotica, Serbia, Sept. 2010, pp. 93–97.
- [2] M. Arrawatia, M. S. Baghini, and G. Kumar, "Broadband Bent Triangular Omnidirectional Antenna for RF Energy Harvesting," *IEEE Antennas Wireless Propagation Letters*, vol. 15, pp. 36–39, 2016.
- [3] S. Sun, G. R. MacCartney, M. K. Samimi, et al. "Synthesizing Omnidirectional Antenna Patterns, Received Power and Path Loss from Directional Antennas for 5G Millimeter-Wave Communications," in *2015 IEEE Global Communications Conference (GLOBECOM)*, San Diego, USA, Dec. 2015, pp. 1-7.
- [4] Y.-M. Cai, S. Gao, Y. Yin, et al. "Compact-Size Low-Profile Wideband Circularly Polarized Omnidirectional Patch Antenna With Reconfigurable Polarizations," *IEEE Transactions on Antennas Propagation*, vol. 64, no. 5, pp. 2016–2021, May 2016.
- [5] B. T. McWilliams, E. E. Schnell, S. Curto, et al. "A Directional Interstitial Antenna for Microwave Tissue Ablation: Theoretical and Experimental Investigation," *IEEE Transactions on Biomedical Engineering*, vol. 62, no. 9, pp. 2144–2150, Sep. 2015.
- [6] Y. Guo and S. D. Prior, "Development of Active Gimbal System for Directional Antenna on a Small Remotely Piloted Aircraft (RPA)," in *RPAS Today - Opportunities and Challenges*, United Kingdom, Jun. 2014.
- [7] E. R. Juma, H. Wijanto, and U. Sunarya, "Implementation and Analysis of System Automatic Tracking Control Performance 433mhz Frequency Receiver Antenna Polarization Based," *e-Proceeding of Engineering*, vol. 2, no. 1, pp. 185–192, 2015.
- [8] S. Jenvey, J. Gustafsson, and F. Henriksson, "A Portable Monopulse Tracking Antenna For UAV Monash UAVs," in *22<sup>nd</sup> International Unmanned air vehicle systems : 22nd International Conference*, Bristol, United Kingdom, 2007.
- [9] M. Kim, J. Kim, and O. Yang, "Precise attitude control system design for the tracking of parabolic satellite antenna," *International Journal of Smart Home*, vol. 7, no. 5, pp. 275–290, 2013.
- [10] Y. Yalçın and S. Kurtulan, "A Rooftop Antenna Tracking System: Design, Simulation, and Implementation," *IEEE Antennas and Propagation Magazine*, vol. 51, no. 2, pp. 214–224, 2009.
- [11] C.-H. Cho, S.-H. Lee, T.-Y. Kwon, and C. Lee, "Antenna Control System using Step Tracking Algorithm with  $H_\infty$  Controller," *International Journal of Control, Automation, and Systems*, vol. 1, no. 1, pp. 83–92, 2003.
- [12] J. M. Lin and P. K. Chang, "Intelligent Pd-Type Fuzzy Controller Design for Mobile Satellite Antenna Tracking System with Parameter Variations Effect," in *IEEE Symposium on Computational Intelligence in Control and Automation (CICA)*, 2011, pp. 1–5.
- [13] S. A. Fandakli and H. I. Okumus, "Antenna Azimuth Position Control with PID, Fuzzy Logic, and Sliding Mode Controllers," in *2016 International Symposium on Innovations in Intelligent Systems and Applications (INISTA)*, Sinaia, Romania, Aug. 2016.